A DIRECT LINK BETWEEN FEATURE TRACKING AND HEIGHT ASSIGNMENT OF OPERATIONAL ATMOSPHERIC MOTION VECTORS

Régis Borde and Ryo Oyama

1 EUMETSAT, Am Kavalleriesand, 31, D-64295 Darmstadt, Germany
2 JMA, 3-235 Nakakiyoto, Kiyose, Tokyo, 204-0012, Japan

Abstract

Height Assignment (HA) is currently the most challenging task in the operational Atmospheric Motion Vectors (AMV) extraction schemes. Several sources of error are associated with the height assignment step, including the sensitivity of the HA methods to several atmospheric parameters. However, one of the main difficulties is to clearly identify the individual image pixels used in the feature tracking process in the tracer box, which in turn are used for the HA calculation. This paper describes a possibility to keep a closer link between the tracking and the HA step, using individual pixel contribution to the cross correlation coefficient to select the pixels used for the height assignment.

INTRODUCTION

Atmospheric Motion Vectors (AMVs) are one of the most important products derived from all geostationary satellites, because they constitute a significant part of the observation data assimilated in Numerical Weather Prediction (NWP) models. Indeed, they are the only upper wind observations with good global coverage for the tropics and mid-latitudes, especially over the large ocean areas. AMVs are routinely extracted by a number of meteorological satellite operators (EUMETSAT, NOAA/NESDIS, Japan Meteorological Agency (JMA)).

For Meteosat Second Generation (MSG), the derivation of displacement vectors is realised by tracking clouds or water vapour features in consecutive Meteosat satellite images. The final hourly AMV product is an average of three vectors calculated from a sequence of four images. The basic elements of wind vector production are (Holmlund, 2000): (a) selecting a feature to track; (b) tracking the target in a time sequence of images to obtain a relative motion; (c) assigning a pressure (altitude) to the vector; and (d) assessing the quality of the vector. The height assignment step, which estimates the cloud top height in case of cloud motion vectors, is still recognised to be the source of largest error in this AMV extraction process. In particular, the pressure associated with the AMV is sometimes higher than the forecast pressure of best correspondence to the detected speed. This situation is especially frequent at high levels, in strong wind shear situations, and can have a negative impact on the forecast issued from NWP models. The operationally used height assignment schemes try to account for semi-transparency, broken cloud fields, multi-layered clouds, and low level targets. The sources of errors (Borde, 2006) include the sensitivity of the methods to local atmospheric parameters (Borde and Dubuisson, 2007). Within all these schemes, the pixels that will be input to the height assignment need to be selected. However, this selection process is not currently done with a direct and clear link to the tracked feature.

At EUMETSAT, AMVs are derived e.g. from tracking clouds in the 10.8 μm IR channel of Meteosat, using a target box size of 24x24 pixels (72x72 km^2 at the sub-satellite point). Various types of clouds can be detected in such a target box, potentially moving at different speeds and altitudes. One of the critical issues is then to select the pixels within in the target box that should be used for the HA calculation. The EUMETSAT cross correlation scheme used for tracking the clouds is mainly based on the maximum contrast criterion, which intrinsically tends to favour the coldest cloudy pixels in the infrared channels. The EUMETSAT height assignment scheme uses a sub-group of the cloudy pixels for the height assignment, considering the coldest peak of the 1-D histogram of cloud top pressures

calculated on a pixel basis in the target box (ASD internal EUMETSAT document). However, this set of pixels selected does not necessarily correspond to those that mostly contribute to the tracking. In this paper the individual pixel contribution to the cross correlation coefficient defined by Büche et al. (2006) is used to illustrate the necessity for considering such information in the AMV HA.

INDIVIDUAL PIXEL CONTRIBUTION TO THE CROSS CORRELATION COEFFICIENT

In the following, the AMVs considered are derived from tracking clouds in the 10.8 µm IR channel of Meteosat-8, using 24x24 pixels target boxes. No filters and/or enhancement process are used in this study. The first step of the AMV extraction scheme is to find a target at a selected grid point. For each location within target search area of 48x48 pixels centred on the grid point, the local mean and standard deviation of 3x3 pixels are computed. The target location is selected to be the 24x24 target box which has the maximum contrast (difference between maximum and minimum local means). Overlap of more than 50% is not allowed between adjacent targets. Initially the scheme will try to find a cloudy target, containing more than 50 pixels classed as cloudy based on MSG cloud mask product. If this is not found, it is selected as a clear sky target.

Thereafter the position that best corresponds to this target is located in the second image, taken 15 minutes later. The search is done in an 80x80 pixel box centred on the target location. A cross correlation method is used to do the matching. The matching compares only the individual pixel counts of the target box with all possible locations of the target box in the search area to find the best match. The degree of matching between pixel radiances a and b between the two images A and B is classically given by the following two-dimensional cross-correlation coefficient:

$$CC(m,n) = \frac{1}{MN}\sum_{i=1}^{M}\sum_{j=1}^{N}\frac{a_{i+m,j+n}-\bar{a}(m,n)}{\sigma_a(m,n)}\frac{b_{ij}-\bar{b}}{\sigma_b} = \sum_{i,j}^{M,N} CC_{ij}(m,n) \qquad (1)$$

where *m*, *n* is the (lines, elements) displacement of the target box in image B from the initial position in the first image A. The correlation coefficient CC(*m*, *n*) is normalized to values between -1 (mirror structures) and +1 (identical structures). The symbols ā and σ_a represent the average and the standard deviation of the radiances a in image A, respectively (correspondingly for b in image B). Values M and N correspond to the box size, MxN=24x24 for this study. According to Büche et al. (2006), the correlation coefficient can also be written following third part of Eq. (1), where the symbol CC_{ij} expresses how much the individual pair of pixels (*i*, *j*) in image1 and (*i*+*m*, *j*+*n*) in image 2, contributes to CC(*m*, *n*).

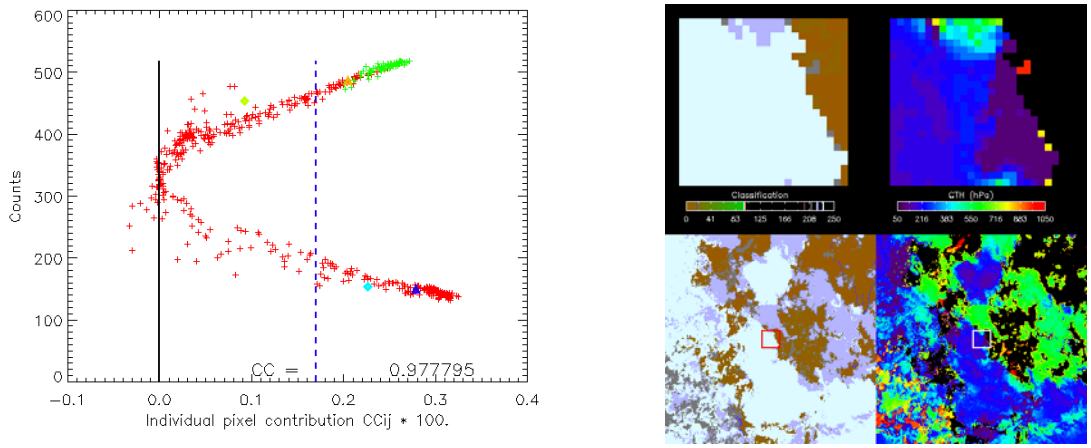

Figure 1: **Infrared counts within the target area are plotted against their individual pixels contribution (left) for the corresponding target area (right). AMV has been extracted using IR10.8 channel of SEVIRI (1st december 2006, 2:00 and 2:15 UTC images)**

Figure 1 illustrates how the individual pairs of pixels taken from the 24x24 pixels target boxes between two consecutive Meteosat-8 images (1st december 2006, 2:00 and 2:15 UTC images), contribute to the maximisation of CC(m,n). Green dots correspond to clear sky pixels, red dots to cloudy pixels

within the target area. The corresponding scene (SCE-CLA) and cloud top height (CLA-CTH) information are plotted on the right side. High levels, mid levels and low levels clouds correspond respectively to clear blue, violet and grey colours. The correlation matching has been done using count values, but radiance can be used indifferently. Usually, coldest and warmest pixels in the target box contribute the most to CC(m,n). In the case of a clear distinction between cold and warm scenes within the target box, the relative individual pixel contributions, CC_{ij}, present a clear 'C-shaped' distribution, as shown in Figure 1. The distance between the two branches corresponds to the contrast of the structures within the target area. Several pixels have a negative CC_{ij}, which generally correspond to pixels that have very different radiative properties but the same position within the two target boxes in the image 1 and image 2. Appearance and/or decay of clouds between image 1 and 2 generally induce such negative CC_{ij}. Pixels that contribute the most to CC(m,n) can be defined as those that have CC_{ij} greater than the average CC_{ij}, $<CC_{ij}>$, figured by the dashed blue line on the figure 1.

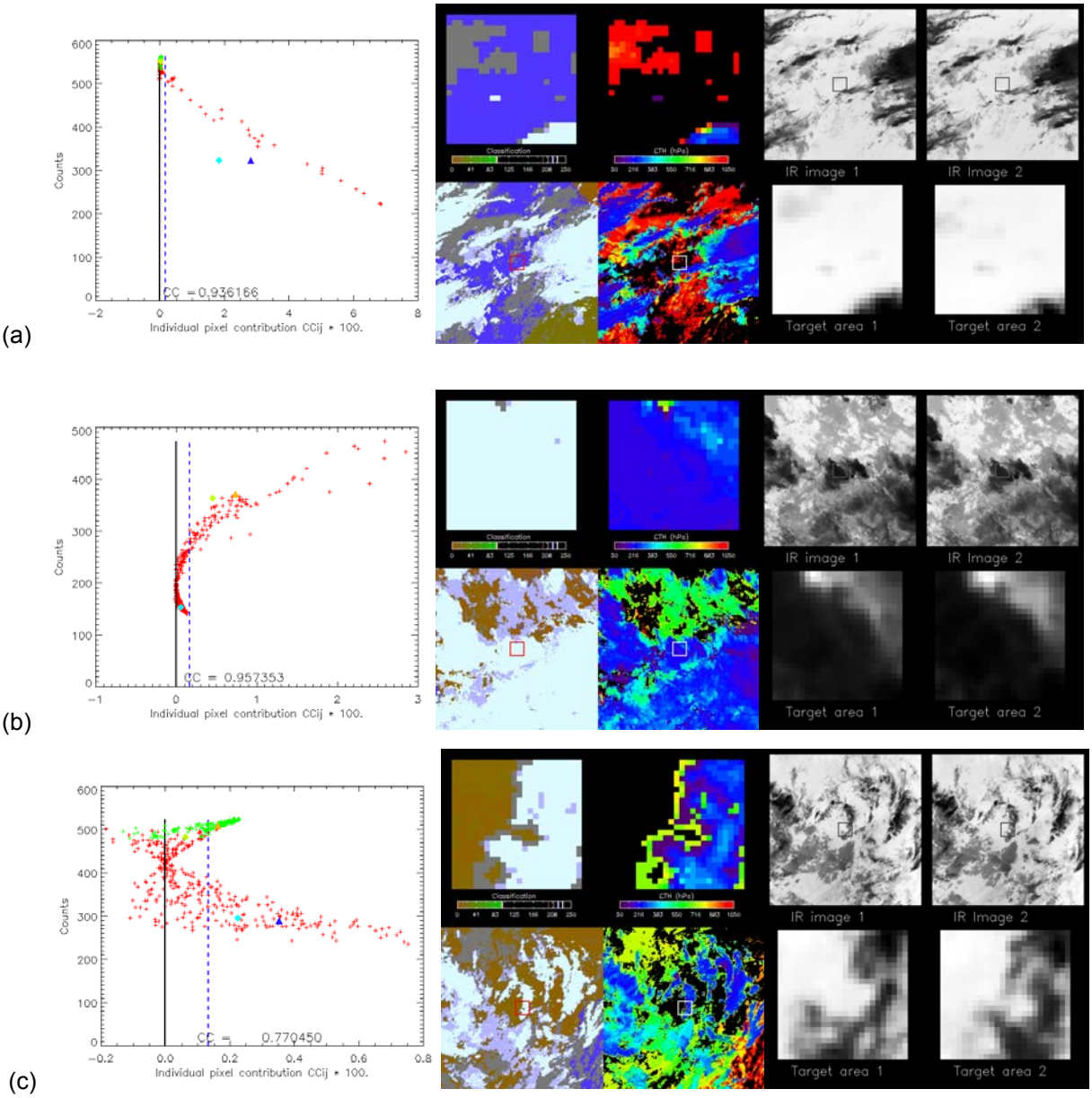

Figure 2: **Various cases encountered at the end of AMV process. Infrared counts within the target area are plotted against their individual pixels contribution (left) ; and presented together with corresponding target scenes and CLA-CTH (middle) and IR10.8 radiance for image 1 and 2 (right).**

The two branches of this 'C shaped' curve are respectively under and above the average count value within the target area. Cloudy pixels also contribute to the warm branch together with clear sky scenes. The cold branch corresponds to cloud top pixels, when the warm branch is composed by clear sky scenes, cloud edges, fractional clouds, semi-transparent clouds and low level clouds in case of multi layer scenes. For each of these branches the group of pixel that contribute the most to CC(m,n) can be selected and considered separately for specific use. An example is given by the blue and orange triangles plotted on Figure 1, which represent the weighted mean count value, balanced by CC_{ij} information, of the pixels that contribute the most to tracking process (CC_{ij} greater than $<CC_{ij}>$) for the cold and warm branches respectively. Clear blue and greenish diamonds represent the same calculations applied to the whole cold and warm branches (CC_{ij} greater than 0), respectively.

However the case presented on the Figure 1 results from a very good correlation example, CC=0.978, and it is not representative of the various types of situation encountered at the end of the AMV tracking process. Plots in Figure 2 illustrate more common and tricky situations, which correspond respectively to cases for which a few of the coldest (respectively warmest) pixels mostly lead to the tracking process, Figure 2a (respectively Figure 2b) and case where large part of the coldest has a negative CC_{ij}, Figure 2c.

Figure 2a corresponds to a multilayer cloudy situation over ocean. The correlation is very good, CC=0.936, and the group of pixels that really drive the tracking process is composed by the high level pixels located at the bottom right of the target box (clear blue in classification picture). They represent a small percentage of the coldest pixels, 6.7%, but their contribution to correlation is very large.

Figure 2b correspond to totally cloudy scene, there is not any clear sky pixel within the target box. The correlation is also very good, CC=0.957. That situation corresponds to the motion of a large homogeneous cloud layer, for which all the coldest cloudy pixels have nearly the same radiative properties and thus a similar, but individually low, contribution to the correlation process. No coldest pixels have a CC_{ij} larger than the average $<CC_{ij}>$, and then the correlation process is now relatively driven by the warmest pixels, which correspond to 'hole' and fractional cloudy pixels.

Figure 2c illustrates the motion of high level clouds over land. Their shapes are changing very much between image 1 and 2, but the general correlation remains good, CC=0.77. However, some of the coldest pixels contribute negatively to CC(m,n) and these 'ghost' cloudy pixels must be eliminated for HA. Although the cross correlation coefficient is in this case smaller, the detected wind can still be used within an operational forecasting system.

The Figure 3 presents the histogram of the percentage of coldest pixels that contribute the most to the tracking (CC_{ij} larger than $<CC_{ij}>$) for a set of 13995 AMVs, tracked using IR10.8 SEVIRI images of the 1st December 2006 at 2:00 and 2:15 UTC. This histogram has been calculated excluding 'ghost' coldest pixels that have a negative CCij, which mainly correspond to appearance and/or decay and/or changes in the cloud shape between the images 1 and 2. Most of the AMVs have been detected using a percentage of coldest pixels ranged between 12 and 20%. However, the peak-width of this histogram is quite large, and does not show as an adequate solution the general use of a fixed percentage of coldest pixels that could be applied to all the situations for future HA calculations.

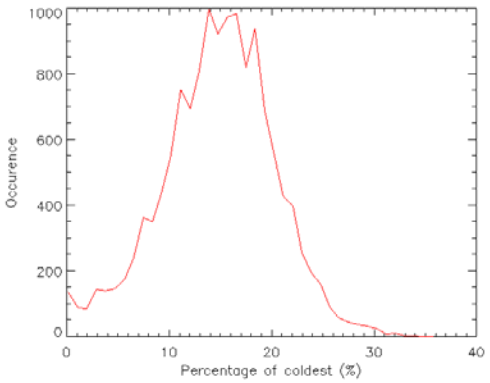

Figure 3: **Histogram of the percentage of coldest pixels that have an individual contribution to cross correlation coefficient greater than the average contribution, for a set of 13995 AMVs (1st December 2006 at 2:00 and 2:15 UTC)**.

ESTIMATION OF THE PRESSURE USING CC_{IJ} INFORMATION.

To estimate the AMV altitude, the satellite operators (EUMETSAT, NOAA/NESDIS, JMA) use several techniques to select the pixels that are used for the HA calculation inside the target box. But none of them currently includes direct information coming from the correlation process. The most common method selects the coldest pixels present in the target box to calculate the height. NOAA/NESDIS uses a fixed threshold of 25% coldest pixels for GOES instrument (Daniels et al., 2002). EUMETSAT uses the coldest peak of the dynamic histogram analysis of CLA-CTH parameter calculated on a pixel basis inside the target area for MSG (ASD internal EUMETSAT document). These CLA-CTH estimations are corrected from semi-transparency effect. JMA uses the most frequent 1-D histogram of cloud top pressures calculated on a pixel basis in the target box for MTSAT (Oyama and Shimoji, 2008). These CTH calculations are corrected from semi-transparency effect. Once the pixels are selected, several methods are used to calculate the altitude of the AMV as function of the cloud type. Opaque cloud heights are estimated from the representative Equivalent Black Body Temperatures. CO2 slicing (Menzel et al., 1983) and WV-IRW intercept method (Schmetz et al., 1993) are used operationally to estimate the cloud top pressure of semi-transparent clouds; both require clear sky and cloudy information present in the target box to estimate the HA. CO2 slicing can be applied on a pixel basis, while WV-IRW is applied on a group or cluster of pixels. The representative cloudy radiance of the cluster generally corresponds to the average radiance of the cloudy pixels that are selected.

Instead of a simple radiance average, the representative clear sky and cloudy radiances can be calculated by weighting the pixel radiances by CC_{ij} and be used as input for the HA methods. Oyama et al. (2008) show some improvements applying this at JMA. However, in the framework of this study we have chosen to use the CLA-CTH parameters calculated on a pixels basis to estimate the pressure. That choice has been guided by the EUMETSAT intention to use its future OCA product (Watts et al., 1998) to estimate the AMV pressure. This one will provide information on cloud top height, cloud fraction, cloud type, droplet size…etc, for every cloudy pixel. As this product is currently under operational implementation and not yet available, the preliminary tests presented below have been done using the classical CLA-CTH product.

Figure 4a,b,c,d show CLA-CTH within the target area plotted as function of CC_{ij} for the same cases figured out in Figure1 and Figure 2a,b c, respectively. Triangle and diamonds correspond now to the weighted pressure calculated from CLA-CTH, balanced by their corresponding CC_{ij}. Dark blue triangle represents the result for the pixels that contribute more than $<CC_{ij}>$ to the correlation coefficient for the coldest branch (cf. Figure 1 and 2), when clear blue diamond is the result for the whole cold branch ($CC_{ij} > 0$). Orange triangle and greenish diamond correspond to the same for warm branch. Error bars represent the corresponding weighted standard deviation, balanced by CC_{ij}. The horizontal dashed line corresponds to the pressure estimated using 25% coldest pixels. Solid red line corresponds to CLA-CTH histogram.

On the Figure 4a the pixels having a CLA-CTH value close to 100 hPa correspond to semi-transparent clouds figured out in violet on the upper right picture of the Figure 1. Their cloud top pressure has been corrected from semi-transparency effect, which explains why they finally get a smaller pressure than coldest opaque pixels within the target box. These pixels are included into the warm branch of the graph in Figure 1, and few of them really contribute to the correlation coefficient. Looking at the Figure 4a it is obvious that a HA technique which uses coldest peak of CLA-CTH histogram should set the AMV pressure slightly too low, and then the cloud top a bit too high in the troposphere, because it mixed together semi-transparent and opaque clouds. The pressures for the cold branch are very close together, respectively 191+/-20 hPa ($CC_{ij} > 0$) and 188+/-16 hPa ($CC_{ij} >$ average). For this case 32% of coldest pixels contributes significantly to the correlation. Pressure estimated from the 25% coldest is equal to 184 hPa. Sometimes, when the warm branch is essentially composed by semi-transparent cloudy pixels, the final pressure for the warm branch can be lesser than the one estimated for the cold branch,

Figure 4b illustrates a case for which small percentage of the coldest pixels, 6.7 %, contribute significantly to the correlation. They are composed of the high levels cloudy pixels located at the bottom right of images in Figure 2a. Unfortunately, there are also low level clouds in the target area, which do not contribute to the tracking but that can be used to set the AMV height. Technique using coldest peak of CLA-CTH histogram should set the correct pressure of the high level clouds, but a technique using 25% of coldest pixels mixed together high level and low level clouds, and place the

cloud top too low at 645 hPa. The most frequent peak of CLA-CTH histogram is composed of low level clouds. The final pressures for the cold branch are respectively 271+/-85 hPa (CC_{ij} > 0) and 268+/-75 hPa (CC_{ij} > average). The multilayer cloudy situation describes here is very frequent.

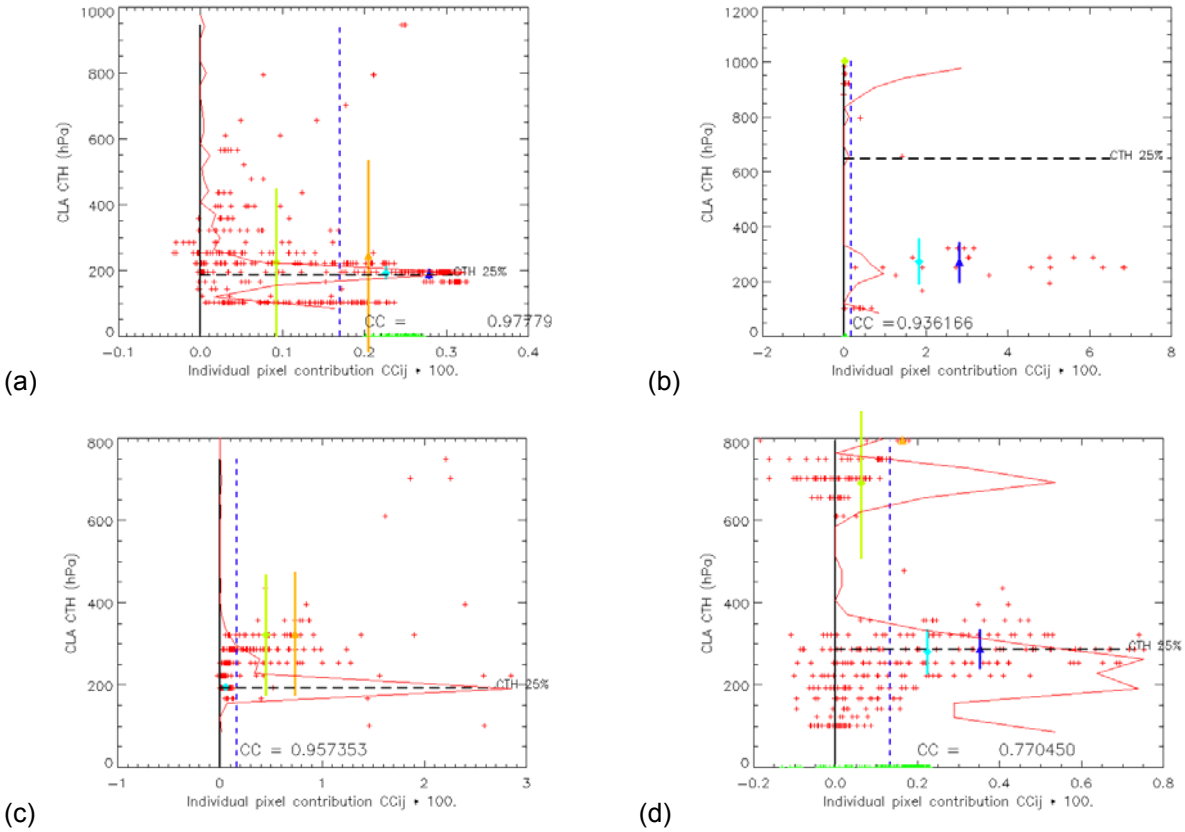

Figure 4: **CLA-CTH within the target area are plotted against their individual pixels contribution. Graphs a,b,c,d correspond respectively to situation already plotted in Figure 1, and Figure 2a,b,c.**

As described above, Figure 4c corresponds to the motion of a large high level cloud layer. The correlation process is then driven by the warmest pixels within the target box, which are mainly composed of cloud edges. Cloud edges and/or holes move at the same speed than the cloud itself. For this situation all the techniques described above give nearly the same results, as the coldest pixels have all the same radiative properties. The final pressures for the whole cold branch is 194+/-8 hPa (CC_{ij} >0) and 192 hPa for the 25% coldest. There is not any cold pixel that contributes more than <CC_{ij}> in that case, and then nearly 50% of the coldest have been used to calculate the pressure of the whole cold branch.

Figure 4d illustrates a case for which the cloud shape has changed very much between the image 1 and 2. However, knowing that the detected speed is fast, 20.5 m/s, a visual inspection on the Infrared images plotted in Figure 2c shows that the position of the target area 1 and 2 are realistic. More than 8% of the coldest pixels have a negative contribution to the correlation coefficient, which means they have mainly appeared or disappeared between images 1 and 2. Excluding them from the selection group of pixel used for the HA, only 19% of the coldest have been considered for the cold branch pressure calculation (CC_{ij} >average), 286+/-48 hPa. Pressure estimated for the whole cold branch is 280+/-55 hPa (CC_{ij} >0) and pressure estimated using the 25% is 286 hPa. The use of the coldest peak of CLA-CTH histogram should set the cloud top slightly too high in that case.

All these examples illustrate the various situations that can be encountered during the AMV extraction process and the inherent difficulty in calculating the altitude of the features that represents the atmospheric motion. A detected motion vector does not necessarily correspond to the displacement of a single cloud layer; it generally represents more an average displacement of cloud segments that are moving at various speeds and altitudes in the target box. The use of CC_{ij} for the final height estimation should enable a dynamic and specific selection of the feature that corresponds the most to the

detected motion. It also allows the derivation of an error bar associated to the AMV pressure, which is a strong request of NWP centres for assimilation. The pressure estimated for the whole cold branch is generally slightly larger than the pressure estimated using only the coldest pixels that contribute to the correlation process more than $<CC_{ij}>$. However that is not always the case and this information could also be used in the future as a flag for very tricky situations and/or big internal variability within the target box.

New possibility to move the position of the final AMV.

The CC_{ij} can also be used at the end of the AMV process to move the position of final AMV from the center of the target box to a more realistic position, corresponding to the position of the feature tracked. Figure 6 shows the histogram of the distance to the center of the target box for the geographical position of various percentages of the coldest pixels within the target box (colored lines), and for the weighted position of the coldest pixels that have CC_{ij} larger than $<CC_{ij}>$ (solid line) and CC_{ij} larger than 0 (dashed line). The distance to the center of the target box is given in pixels. Using 24x24 target boxes, the largest possible distance to target center is nearly 17 pixels. The peak of the histogram is around 10 pixels for black solid line, which represents 30 km at nadir. It has to be noted that coldest pixels are generally located far from the center of the target box, as illustrated in Figure 2a as well. The place of the final AMV at the location of the tracked feature is of course important for comparison against forecast and radiosonde observations, but also to plot the AMVs on maps. Indeed there are many cases where no clouds are present at the center of the target box and the detected AMV is plotted over clear sky area.

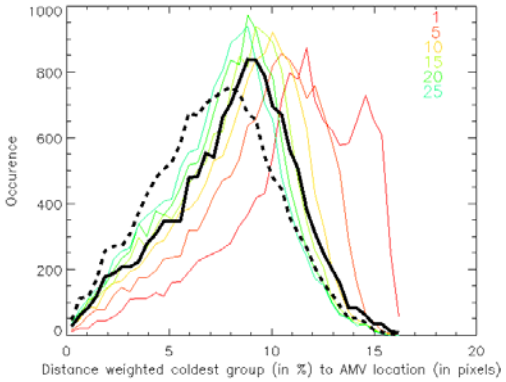

***Figure 6*: Histogram of the distance of various percentages of coldest pixels to the center of the target box. Black lines correspond to the distance of the cold branch positions ; considering pixels that have CC_{ij} larger than $< CC_{ij} >$ (solid line) and larger than 0 (dashed line). (1st December 2006 at 2:00 and 2:15 UTC).**

CONCLUSION

Accurate calculation of the AMV pressure is sensitive to the selection of the pixels used for the cloud top height estimation. Results presented in this paper show that both coldest and warmest pixels generally lead the tracking process through the cross correlation algorithm. Various situations are described, showing that the current use of a fixed percentage of coldest pixels for the cloud top height estimation appear to be not realistic all the time. The technique using the histograms of CLA-CTH appears also limited in tricky situations, due to the presence of cold opaque pixels and corrected semi-transparent pixels within the same coldest peak. A process that includes CC_{ij} information then could be very helpful to improve the HA estimation.

Several ways to incorporate this information into the various existing HA schemes are under study. Use of weighted representative radiance, balanced by CC_{ij} is presented by Oyama et al (2008). The technique proposed above uses the existing CLA-CTH parameter in conjunction with CC_{ij} information. This technique should probably not solve all the HA tricky problems encountered in operational AMV extraction, but it should improve the overall consistency of the AMV algorithms, preserving the essential link between altitude estimation and feature tracked. This link is ensured through sound mathematical and physical properties related to the correlation scheme itself. It is of course assumed

that CLA-CTH product is good quality and gives a correct estimation of cloud top height. Seze et al. (2008) compared CLA-CTH product present within the AMV target box against CALIOP measurements and showed a general good agreement between the two. An 'Optimal Cloud Analysis' scheme is now under development at EUMETSAT (Watts et al., 1998) with the aim to accurately estimate the cloud top height. Such new product should then be used adequately in the future to again increase the performance of that technique. However, this method needs to be tested over a long period in operational environment, compared with radiosonde and the new AMV pressures assimilated in NWP models for testing. Even if recognised as an important issue, the HA is not the only one problem related to AMVs. How the detected motions and speeds are representative of the local winds is also a big issue (Velden and Bedka, 2008 ; von Bremen et al., 2008). The method described here does not get any answer to this last question, but it ensures that the altitude of the 'detected motion' is estimated on the correct feature/pixels, using as best as possible the techniques currently available.

REFERENCES

ASD; 'MSG Meteorological Products Extraction Facility Algorithm Specification Document' edited by EUMETSAT. Reference: EUM.MSG.SPE.022

Borde, R. and Ph. Dubuisson, (2007), 'Cloud top height estimation using simulated METEOSAT-8 radiance', *Procs. SPIE*, in press.

Borde, R., (2006), 'AMV height assignment methods with Meteosat 8', *Proc. Eighth Int. Winds Workshop*, Beijing, China, EUM P-47.

Büche, G. H. Karbstein, A. Kummer and H. Fischer, (2006), Water Vapor Structure Displacements from Cloud-Free Meteosat Scenes and Their Interpretation for the Wind Field. *J. Appl. Meteor*., *45*, 556-575.

Daniels, J., et al., 2002: Status and development of GOES wind products at NOAA/NESDIS, Proceedings of 6th International Winds Workshop, EUMETSAT, 71-80.

Menzel, W.P., W.L. Smith and T. Stewart, (1983), 'Improved cloud motion wind vector and altitude assignment using VAS'*, J. Climate Appl. Meteor.*, *22*, 377-384.

Oyama, R., R. Borde, J. Schmetz, T. Kurino, (2008), Development of AMV height assignment directly linked to feature tracking at JMA, *Proc. Ninth Int. Winds Workshop*, Annapolis, USA, (this issue)

Oyama, R. and K. Shimoji, 2008: Status of and future plans for JMA's Atmospheric motion vectors, Proceedings of 9th International Winds Workshop.

Schmetz, J., K. Holmlund, J. Hoffman, B. Strauss, B. Mason, V. Gaertner, A. Koch and L. van de Berg, (1993), Operational cloud motion winds from METEOSAT infrared images. *J. Appl. Meteorol*., *32*, 1206-1225.

Sèze, G., S. Marchand, J. Pelon, R. Borde, (2008), A Comparison of AMV cloud top pressure derived from MSG with space-based Lidar observations, *Proc. Ninth Int. Winds Workshop*, Annapolis, USA, (this issue)

Velden, C., and K. Bedka, (2008), Identifying the uncertainty in determining satellite-derived AMV height assignments, *Proc. Ninth Int. Winds Workshop*, Annapolis, USA, (this issue)

von Bremen, L., N. Bormann, S. Wanzong, M. Hortal, D. Salmond, J.-N. Thépaut, Peter Bauer, (2008), Evaluation of AMVs derived from ECMWF model simulations, *Proc. Ninth Int. Winds Workshop*, Annapolis, USA, (this issue)

Watts P., C. Mutlow, A. Baran, and A. Zavody. Study on Cloud Properties derived from Meteosat Second Generation Observations. EUMETSAT technical report, 344 pp., 1998